Pergamon

PII: S0301-9322(97)00010-4

Int. J. Multiphase Flow Vol. 23, No. 5, pp. 945–965, 1997

Printed in Great Britain
0301-9322/97 $17.00 + 0.00

DEVELOPMENT OF DIGITAL IMAGE ANALYSIS TECHNIQUES FOR THE STUDY OF VELOCITY AND VOID PROFILES IN SLUG FLOW

M. GOPAL and W. P. JEPSON

NSF, I/UCRC Corrosion in Multiphase Systems Center, Department of Chemical Engineering, Ohio University, Athens, OH 45701, U.S.A.

(Received 12 July 1995; in revised form 5 March 1997)

Abstract—This paper describes the development of a nonintrusive flow visualization method for the quantitative study of the dynamic velocity and void profiles across the pipe cross section in slug flow. The method utilizes novel digital image analysis and computer graphics techniques. Slug flow in a 75 mm diameter, 10 m long Plexiglass pipe is recorded on video using super-VHS cameras and an audio-visual mixer. Sixty images are obtained every second and these are digitized and analyzed on a SGI® graphics workstation. Detailed information regarding the local velocity and void distribution is obtained from the analysis and is used to generate velocity and void profiles across the pipe at different distances into the slug.

Results show that gas is released into the slug in the form of pulses of bubbles resulting in the existence of large, frothy, highly aerated structures in the mixing zone. The hydrodynamic boundary layer is destroyed at the slug front but begins to redevelop in the mixing zone. It becomes fully developed at the end of the mixing zone and the one-seventh power law profile for velocity profile is applicable. At the end of the mixing zone, the gas moves towards the top of the pipe and the void fraction distribution tends to a steady profile. A process dynamic model is developed to predict the variation of the average liquid holdup within the slug. © 1997 Elsevier Science Ltd.

Key Words: image analysis, velocity and void profiles, slug flow, modeling

1. INTRODUCTION

The future production of offshore oil and gas is expected to be from natural sources located in water depths of 500 m or more (Fairhurst 1988). There is a considerable incentive to reduce platform size and cost by employing minimum processing or by dispensing with a fixed platform altogether. Increasing use of subsea technology is already occurring, with a goal of maximum offshore production with onshore processing.

Multiphase transportation is central in these technological developments. The accurate prediction of multiphase flow characteristics in the flowlines is essential for the required design, and safe operation of these pipelines.

An important problem in these long distance multiphase transportation systems is the internal corrosion of the pipeline due to the severe service environment. Carbon dioxide from the produced gas combines with produced water to form carbonic acid which attacks carbon steel flowlines. Generally, corrosion inhibitor applications are designed to combat this problem. The effectiveness of the inhibitors depend critically on the instantaneous phase distribution and velocity in the pipe.

Different flow patterns are observed in multiphase flow at different velocities, for example, stratified, intermittent, and annular flows. The production rates of the oil wells are such that the flow lines are expected to be in slug flow for some time in their lives. This is a highly turbulent flow regime, leading to increased pipe damage from internal corrosion and mechanical impacts. The presence of slug flow in pipelines can significantly reduce the effectiveness of inhibitors.

A profile of a typical slug is shown in figure 1. Waves formed on the liquid film grow to bridge the pipe, causing the liquid film to be accelerated by the gas. As the slug front moves through the pipe, it overruns low moving liquid film ahead of it and accelerates it to the velocity of the slug. A mixing vortex is created and this leads high rates of shear at the pipe wall. Also, as the liquid

is scooped up into the slug, the leading edge of the slug jumps to the top of the pipe and entrains considerable amounts of gas in its wake. This leads to the creation of a highly frothy turbulent region behind the slug front called the mixing zone.

The liquid and gas are assimilated into the slug and accelerated to its velocity. The gas is released in the mixing zone in the form of pulses of bubbles (Jepson 1987). These bubbles are trapped by the mixing vortex and forced towards the bottom of the pipe, where they can impact and collapse. The high rates of shear due to the mixing vortex and the bubble impact and collapse can reduce the protection by an inhibitor film that might have otherwise formed on the pipe wall. Beyond the mixing region of the slug, the level of turbulence is reduced, and buoyancy forces move the gas towards the top of the pipe. The cross sectional area available for liquid flow increases and its velocity decreases; this is the slug body. Eventually a point is reached where the liquid velocity is no longer sufficient to sustain the bridging of the pipe, and the slug falls away. This is called the slug tail. The liquid velocity decreases in the liquid film, its height rebuilds, with waves forming on its surface and the next slug is initiated.

It is of great importance to understand the detailed mechanisms involved in slug flow. Several studies have been conducted to gain a better understanding of the characteristics of this flow regime but knowledge about the detailed features are still lacking. Dukler and Hubbard (1975) showed that slug flow was characterized by sixteen variables, many of which were time dependent. Mathematical models that describe the relationship between different variables have been developed as knowledge of slug flow features have increased over the last decade. However, a detailed understanding of the motion of gas and the distribution of phases within the slug is not known. These are essential for the development of a complete mathematical model to predict slug length and related features.

Maron *et al.* (1982) derived a model for slug flow based on new concepts of periodic distortion of the hydrodynamic boundary layer within the slug front, followed by a recovery process in the body of the slug. They proposed a one-seventh power law velocity profile within the boundary layer. This was later used by Dukler *et al.* (1985) in the development of a physical model for the prediction of the minimum stable slug length. However, this model has not been experimentally confirmed. Jepson (1987) made velocity profile measurements in a 10 cm i.d. pipe, using a stationary slug in an air–water system. He found that, at a distance of 19 cm from the slug front, the incoming liquid was still affecting the flow within the slug. At a distance of 31 cm from the front, the flow was more uniform but the profile was influenced by the distribution of gas bubbles. Increasing the liquid velocity did not affect the profile near the slug front but farther downstream of the jump, the velocity profile became flat. This study made it clear that there was significant

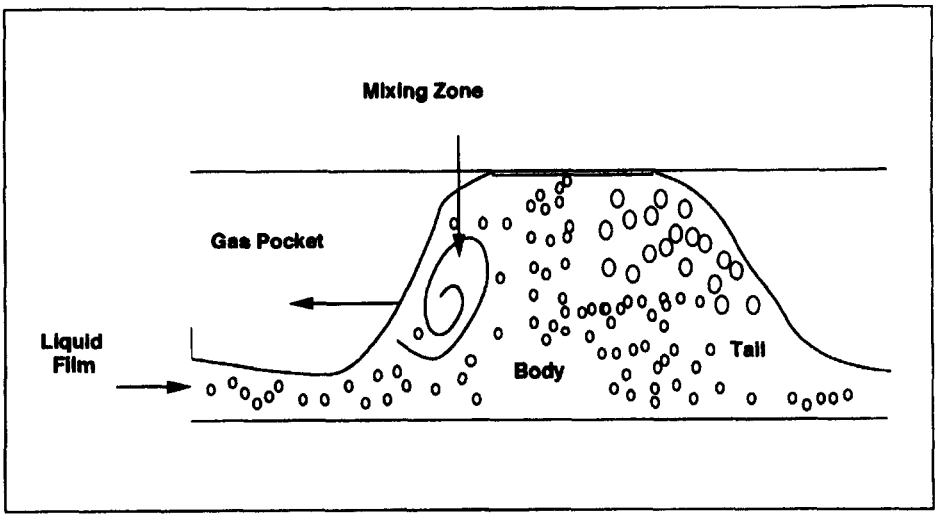

Figure 1. Profile of a slug.

interdependence between the local velocity and void profile within the slug and that this was a function of the slug velocity.

Several studies have been conducted to determine holdup in slugs. Gregory *et al.* (1978) proposed an empirical correlation for liquid holdup in the slug. Based on experiments in 2.5 and 5 cm pipes, they proposed the following correlation

$$1 - \epsilon_S = \frac{1}{1 + \left(\frac{v_S}{8.66}\right)^{1.39}}, \qquad [1]$$

where ϵ_S is the void fraction in the slug, and v_S is the slug velocity. This correlation is widely used in industry. However, it does not predict the liquid holdup (void fraction) in the slug for high viscosity liquids. It was suggested that a modification was necessary to include pipe diameter and fluid property effects in this correlation.

Barnea and Brauner (1985) proposed a physical model for the prediction of void fraction in slugs for horizontal and vertical pipes. They proposed that the gas in slugs was distributed in the form of dispersed bubbles, determined from a balance between breakage forces due to turbulence and coalescence forces due to buoyancy and surface tension. They used conditions proposed by Taitel and Dukler (1976) for horizontal pipes and by Barnea *et al.* (1982) for vertical pipes, for transition between bubble flow and slug flow, to predict the void fraction. The model is seen to work for slug flow and low velocity slugs. At higher velocities, the assumption that the turbulence in the slug is the same as in the dispersed bubble flow is not correct and causes the model to under predict the void fraction in the slug.

Andreussi and Bendiksen (1989) proposed a correlation for air–water slug flow in horizontal and near horizontal pipes using a conductance probe technique. They conducted experiments in 5 and 9 cm i.d. pipes, with inclinations ranging from $-3°$ to $+0.5°$ and used this data along with those of Gregory *et al.* (1978) and Ferschneider (1983), to formulate the correlation. It had provisions to allow for the effect of pipe diameter, inclination and fluid physical properties. An update of that model was proposed by Andreussi *et al.* (1993) where the radial void fraction distribution and size of bubbles were also reported. They found that at the end of the mixing zone the gas tended to move towards the top of the pipe resulting in a higher void fraction at the top. The average gas bubble size was below 5 mm.

Kouba (1986) conducted slug holdup experiments in a 10 cm diameter pipe. The liquid holdup in the slug was found to be a strong function of the slug velocity but was not uniquely dependent on it. The holdup decreased approximately linearly with increasing slug velocities.

Jepson and Taylor (1988) carried out liquid holdup measurements for air–water slugs in a 300 mm i.d. pipeline. They found a strong dependence of liquid holdup on pipe diameter. As the superficial gas velocity was increased to 5 m/s, the holdup decreased to 0.45. There was a limiting holdup value of 0.38 at very high gas velocities. This value was much lower than those predicted by Gregory *et al.* (1978) and for other small diameter pipes. There was a negligible effect of the pipe diameter on the liquid holdup in the slug body below a gas velocity of 3 m/s.

Jepson (1987) used a hydraulic jump to form a stationary slug in a 10 cm horizontal pipe for an air–water system. This method allowed the insertion of a pitot tube and sampling probe to measure holdup without seriously affecting the flow. Local liquid holdup profiles at different locations within the slug were obtained and good agreement with the average liquid holdup predicted by Gregory *et al.* (1978) was achieved. Jepson found that the gas was reasonably well mixed at a distance of 19 cm from the slug front. However, at a distance of 30 cm from the slug front, there was no gas in the lower third of the pipe cross section, while the void fraction near the top of the pipe rose to about sixty percent.

Kouba and Jepson (1987) conducted experiments with stationary slugs in a 15 cm pipeline with air and water for the gas and liquid phases. They defined a Foude number of the film ahead of the slug, and found that the liquid fraction in the slug decreased approximately linearly with increasing Foude number.

In the present study, flow visualization techniques are developed to conduct a detailed analysis of the local characteristics within slugs. The flow is recorded on video and the images digitized on

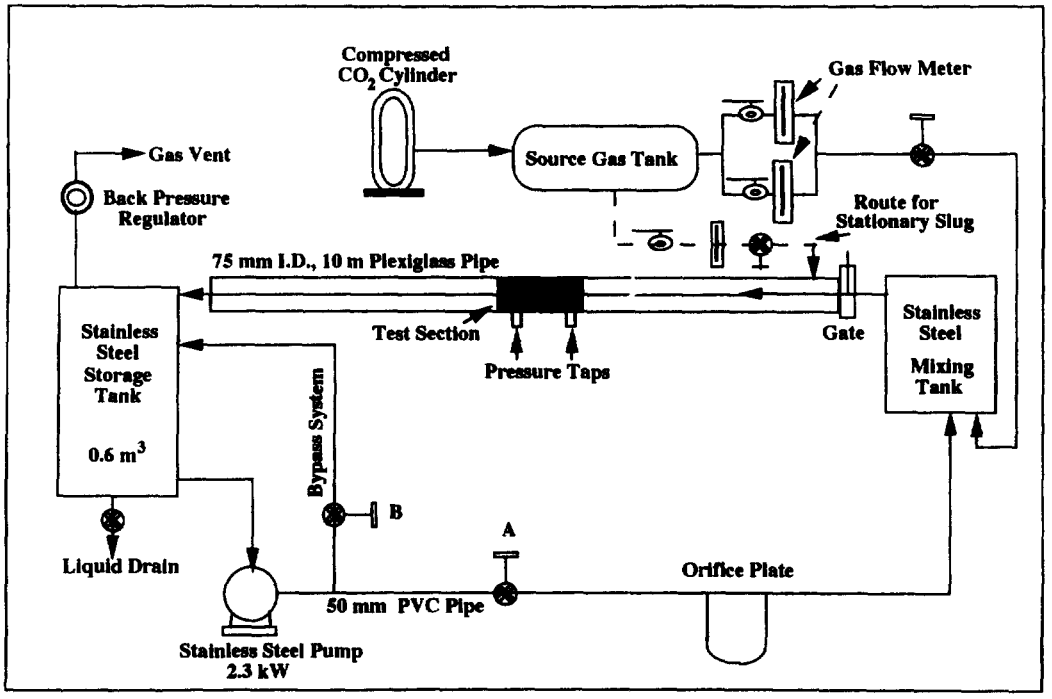

Figure 2. Schematic diagram of experimental setup.

a computer. Digital image processing techniques are then used to perform quantitative analysis of the images to obtain data on velocity and void distribution across the pipe section at different distances into the slug. Mathematical models are then developed to predict the velocity and void profiles in the different regions of the slug.

2. EXPERIMENTAL PROCEDURE

Figure 2 shows a schematic view of the experimental setup used in this study. Liquid is pumped by a 2.3 kW stainless steel centrifugal pump, from a 0.6 m^3 stainless steel storage tank, into a 50 mm i.d. PVC pipe, where its flow rate is measured using an orifice plate. The flow rate of the liquid is controlled by a by-pass system. Carbon dioxide from compressed cylinders is stored in a 1.67 m^3 carbon steel tank at a pressure of 1300 kPa and introduced into the system at an inlet pressure of 800 kPa. The gas flow rate is monitored by Omega FL 4000 Series variable area gas flow meters and is controlled by a flow regulating valve.

The gas and liquid are introduced into a 0.015 m^3 stainless steel mixing tank, and the two-phase mixture is allowed to flow out into the 0.75 m, 10 m long Plexiglass pipeline. The mixture flows back into the liquid storage tank and is separated by means of a specially designed de-entrainment table. The gas is vented to the atmosphere and the liquid is recirculated into the system. Table 1 lists the liquids used, their properties, and the range of variables studied. The range of velocities covered the entire slug flow regime. All of the above values are listed for 298 K and 101.3 kPa.

Table 1. Test matrix for experimental slug flow study

Variable	Deionised water	ARCOPAK90	Carbon dioxide
Density (kg/m^3)	998	850	1.9
Viscosity (Pas)	0.0010	0.015	0.000015
Surface tension (N/m)	0.070	0.040	—
Superficial Velocity (m/s)	0.2–1.3	0.16–0.88	1–5

Figure 3. Three dimensional view of slug flowing in a pipe.

2.1. *Flow visualization system*

The flow was recorded using two cameras at right angles to the flow. A Panasonic WV-D5100, super-VHS camera was used for a closeup view of slug flow features and to obtain detailed data regarding slug flow characteristics, such as, the local velocity and void distribution.

To obtain a high resolution image, a shutter speed of 1/1000 s was used with standard S-VHS resolutions. A 600 watt Smith–Victor fluorescent lamp was used to illuminate the system.

The video outputs from both cameras were connected to a Panasonic WJ-MX12 digital color audio-visual (AV) mixer, with a built-in frame synchronizer. This resulted in high quality, high resolution video images on a single screen that could be used for subsequent analysis. The video signal from the AV-mixer was sent to a Panasonic AG-1960, Hi-Fidelity, industrial Super-VHS video cassette recorder (VCR) equipped with a super-still playback mode. This feature allowed sixty images to be obtained each second using single frame advance.

The video signal from the VCR was connected to a SONY PVM-1341Q Trinitron S-VHS, Hi-fidelity TV monitor and final adjustments to camera positions and image quality were accomplished by examining the picture on this monitor.

The video images were digitized on a Gateway 2000 486-DX2 50 PC using a frame-grabber and software from Digital Vision, MA. The digitized images were finally transferred to a SGI™ Indigo Elan graphics workstation for analysis. The SGI™ has several hundred graphics modules (subroutines) as part of a Graphics Language (GL) software package. These modules were modified and customized for image analysis studies.

All image analysis was performed on video of water-carbon dioxide moving slugs due to the need for high-resolution, clear images that would lend themselves to this type of analysis. For calibration purposes, a cm-ruler was also recorded on tape during each video session. This allowed the pixel co-ordinates obtained from subsequent image analysis to be converted to cm. In this manner, all screen resolutions in the video could be scaled to real-world values.

2.2. *Image analysis procedures*

A manual edge tracking technique was used for the image analysis. An algorithm was developed that allowed the computer to record the coordinates of any desired point in the image by linking the cursor on the screen to the movement of a mouse which was controlled manually.

Programs were written to analyse the images and obtain the local velocity and void distribution. The scheme involves the creation of a buffer in memory for the display of the image, setting the image size and other relevant parameters, and then drawing the image on the screen. A mesh is

then drawn over the pipe cross section, dividing it into ten segments at equal intervals along the diameter of the pipe. Finally, the appropriate subroutine is used to accomplish the necessary edge tracking.

Figure 3 shows a three dimensional image of a slug flowing in the pipe. To accurately analyze this highly turbulent slug, a three-dimensional mesh would have to be created as shown in figure 4 and superimposed on the slug image. It was found that accurate analysis of this image was extremely difficult due to the turbulence. Hence a two-dimensional analysis was carried out using the video image at right angles to the flow. Jepson (1987) in his experiments on stationary slugs, successfully used a division of ten sections across the cross area of the pipe for determining void and velocity profiles. Consequently this number was chosen as the appropriate number of sections.

Figure 5 shows an example of the images used for the analysis. The time-interval between the consecutive images is 0.017 s. This corresponds to the sixty images obtained per second from the video.

Velocity profiles. Figure 5 shows how the boundaries of the gas pockets and individual gas bubbles can be used to generate a velocity profile across the pipe cross section, if no-slip conditions are assumed locally between gas and liquid. Each bubble/gas pocket moves a particular distance between each image shown by the crosses at each section in figure 5(a)–(d). Tracking a single bubble over several images and calculating the distance it has moved, allowed the local velocity to be determined, since each image corresponds to 1/60 th of a second. In most cases the tracking was accomplished over four images as this was the maximum number of images that the bubble was in view. By tracking bubbles at various heights from the bottom of the pipe, velocity profiles across the section of the pipe were generated.

To understand the flow mechanisms at different points in the slug, velocity profiles were generated at the slug front, at the end of the mixing zone, in the slug body, and at the slug tail. These correspond to 0, 20–30, 45 and 60–80 cm from the slug front, for the slug velocities studied.

There are two components to the bubble velocity, axial and transverse. The axial velocity of the bubbles can be equated to the local liquid velocity if there is no slip between the gas bubbles and the liquid locally. In this way, a velocity profile for the liquid can be generated from a corresponding profile for the bubbles. In addition, it is possible to obtain a transverse velocity component for the bubbles, since there is a buoyancy force acting on the bubbles.

From the coordinates of the bubbles in each image, the axial and transverse velocities may be

Figure 4. Three dimensional view of 10-section mesh drawn over pipe for image analysis.

(a)

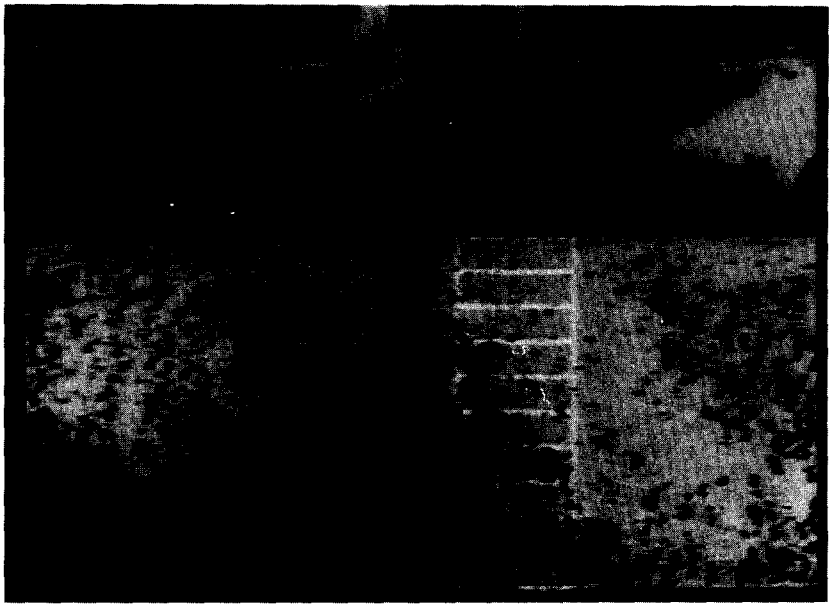

(b)

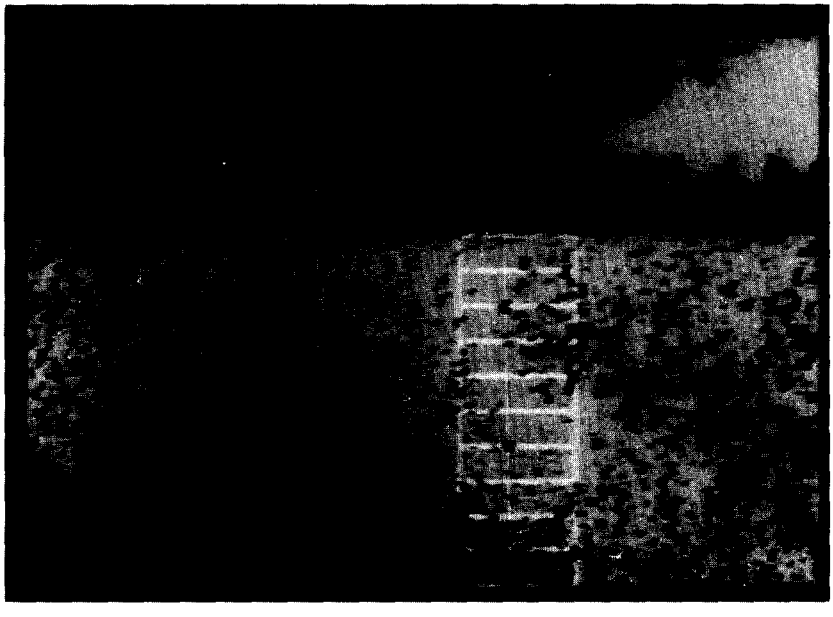

Figure 5. (a) and (b)—*Continued overleaf.*

calculated as follows

$$v_x(h) = \sum_{i=1}^{n} \frac{x_i(h) - x_{i+1}(h)}{c_v(n-1)100}, \quad [2]$$

$$v_y(h) = \sum_{i=1}^{n} \frac{y_{i+1}(h) - y_i(h)}{c_v(n-1)100}, \quad [3]$$

where $v(h)$ is the velocity at height h from the bottom of the pipe along the vertical axis, and $x(h)$ and $y(h)$ are the coordinates of the bubble.

Once the local transverse velocity was calculated, an average rise velocity for the bubbles, v_r, was calculated. The axial distances are measured from left to right in the image.

Void fraction data. No information regarding the void fraction distribution in moving slugs is

(c)

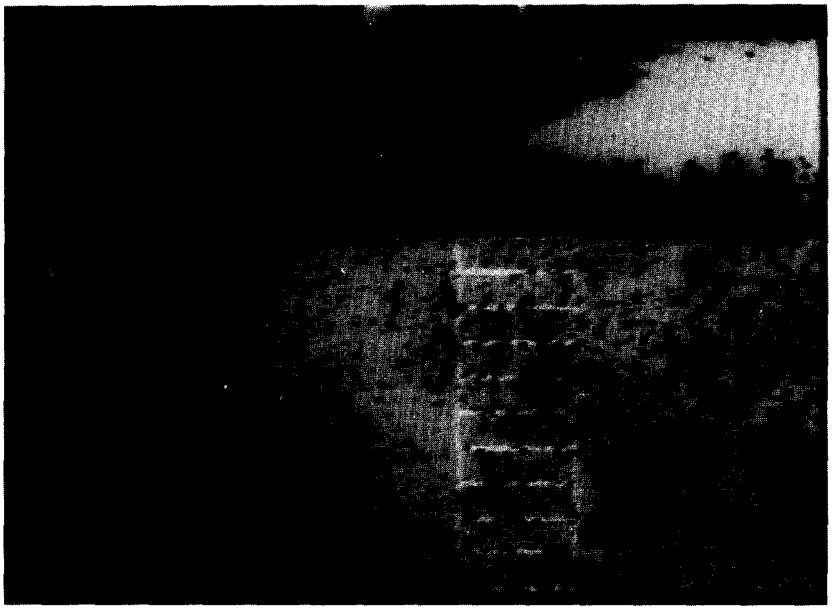

(d)

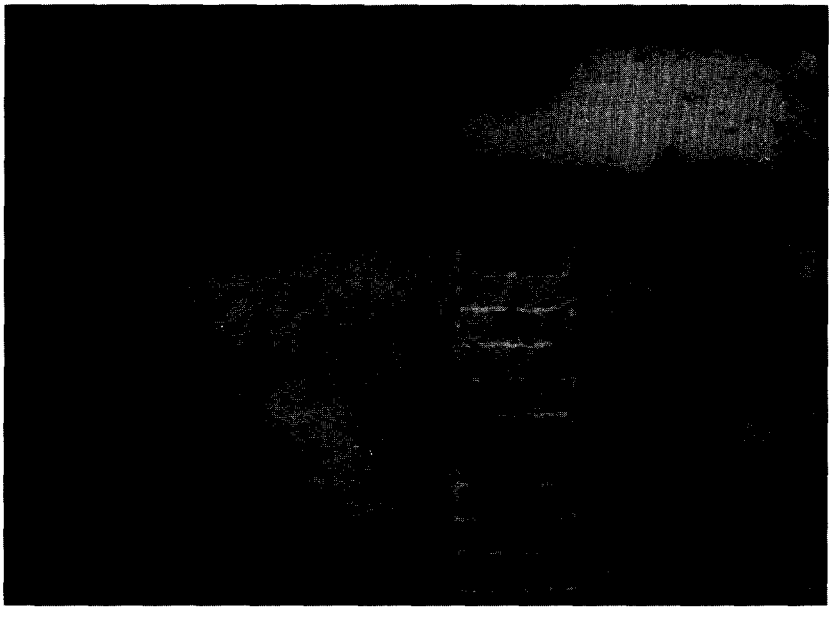

Figure 5. (c) and (d).

currently available. Hence, a detailed void fraction profile across the cross section of the pipe throughout the slug was generated. Typically, this involved the generation of void fraction distribution profiles every 5–10 cm within the slug.

Figure 6 shows video images of the two different types of void structures in a typical slug. In the mixing zone, there is a great deal of turbulence, and the gas and liquid are well mixed. In this region, the voids are large frothy structures covering the entire cross section of the pipe (described as Type B).

At the end of the mixing zone, the gas is pushed towards the top of the pipe due to buoyancy forces. The degree of turbulence is reduced here and the gas is distributed in the form of bubbles in the liquid. These are the kinds of voids that occur mostly in the slug body (described as Type A). The mixing zone is discussed in detail elsewhere (Gopal *et al.* 1995).

For Type B void structures, the area of the face seen from the front was first calculated. Since the void is uniformly distributed throughout the depth of the cross section, its volume of was

obtained by multiplying the face area by the depth of the pipe at that height. This is given by the chord length across the mesh section and is calculated at the middle point of a particular section. The height h, of the middle point of a section is given simply by, $h_2 - h_1$, where h_1 and h_2 are the lower and upper bounds of that section. Once h is known, the chord length, T, is calculated as

$$T = D\sqrt{1 - (2\bar{h} - 1)^2}. \quad [4]$$

The front face area as seen by the camera is calculated from the coordinates (x_i, y_i) of the boundary points of the void profile as follows

$$A_f = \sum_{i=0}^{n-1} x_i \cdot y_{i+1} - x_{i+1} \cdot y_i. \quad [5]$$

(a)

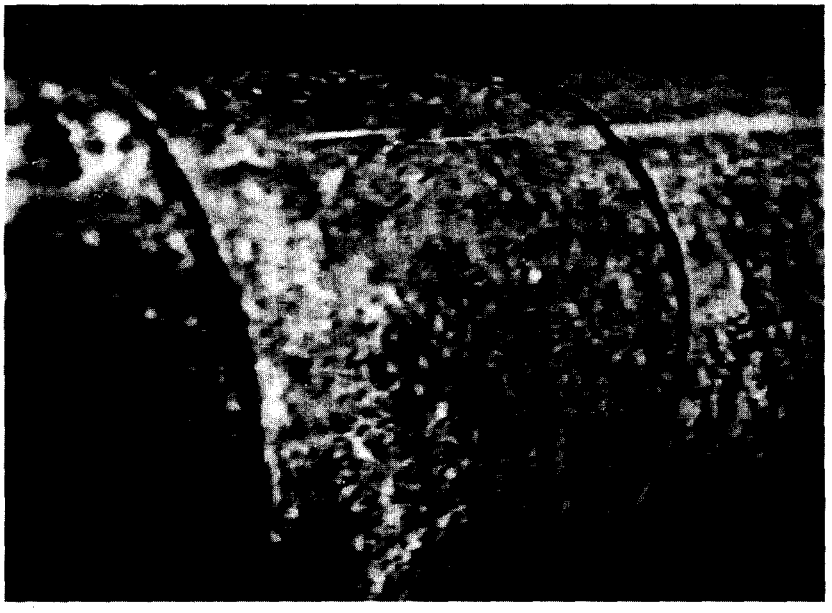

(b)

Figure 6. (a) Video image of void structure in mixing zone of slug (Type B). (b) Video image of void structure in slug body (Type A).

The volume of the Type B void structure is then given by the product of [4] and [5].

Since most of the Type A voids are spherical bubbles, the volumes of these bubbles were calculated using the formula for the volume of a sphere. The face area of each bubble was calculated using [5]. The radius of the sphere was then calculated from this projected area and the volume of the sphere was generated.

Next, the volume of each section of the mesh was calculated. The area of any section of pipe at height h from the bottom can be calculated as follows

$$A = \frac{D^2}{4}\left[\pi - \cos^{-1}(2\bar{h} - 1) + (2\bar{h} - 1)\sqrt{1 - (2\bar{h} - 1)^2}\right]. \quad [6]$$

The face area of section 1 at height h_1 and the cumulative areas of sections 1 and 2 (height h_2) can be calculated using [6]. The area of section 2 is then obtained by subtracting the area of section 1 from the cumulative area. The areas of all ten sections of the mesh can be obtained in this manner. The volume of each section is then the product of its area and the length of the mesh.

Knowing the volume of each section of the mesh and the void volume in each section the void fraction profile can be calculated. The average void fraction is then simply the ratio of the total void volume to the total volume of the cylindrical mesh.

3. RESULTS AND DISCUSSION

3.1. *Velocity profiles*

Figure 7 shows the velocity profiles at various distances into the slug for a superficial liquid velocity of 0.2 m/s and a superficial gas velocity of 1.07 m/s. Figure 7(a) shows the profile at the slug front. It is seen that the high degree of turbulence there, results in a virtually flat velocity profile with a range from about 1–1.3 m/s across the pipe cross sectional area.

Figure 7(b) and (c) show the velocity profile 20 cm and 45 cm into the slug. At 20 cm into the slug, it is seen that a boundary layer is developing with a maximum velocity of 1.3 m/s being at the center of the pipe. At 45 cm into the slug, figure 7(c) shows that the boundary layer is now well established. The profile is similar to that at 20 cm, with a maximum velocity of about 1.2 m/s near the center. Video images indicate (Gopal *et al.* 1995) that at this slug velocity the mixing length of the slug is about 20 cm. Figure 7(d) shows the velocity profile at the slug tail. In this case, the velocity profile has not changed substantially, indicating the maintenance of fully developed flow at the tail of the slug.

The velocity profiles at other superficial gas and liquid velocities were similar to those shown here.

From the above analysis, it may be said that a fully developed boundary layer profile is a reasonable assumption for the velocity profile in the slug body after the mixing zone. This profile begins to distort at the tail end of the slug due to the effects of the gas pocket behind the slug. Hence, a mechanistic profile may be assumed for the velocity in the slug from the end of the mixing zone. Dukler *et al.* (1985) used a one-seventh power law profile to describe the velocity profile in the slug. The law is written as

$$v(y) = v_0\left(\frac{y}{\delta}\right)^{1/7}. \quad [7]$$

It is seen that at the end of the mixing zone, the profile can be assumed to be fully developed, and the thickness of the boundary layer, δ, is equal to the radius of the pipe. The centerline velocity, v_0, in all the above cases, is very close to the slug velocity v_S, which is obtained by summing the superficial gas and liquid velocities in each case (Jepson 1989). This result supports the assumptions made by Dukler *et al.* (1985).

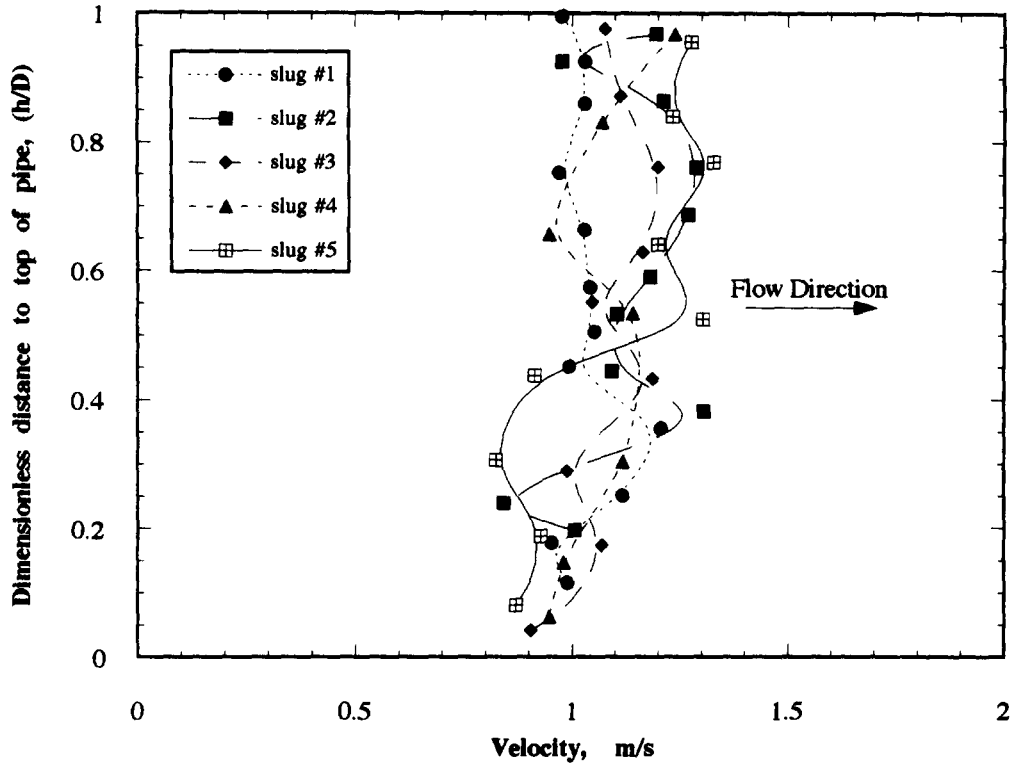

(a)

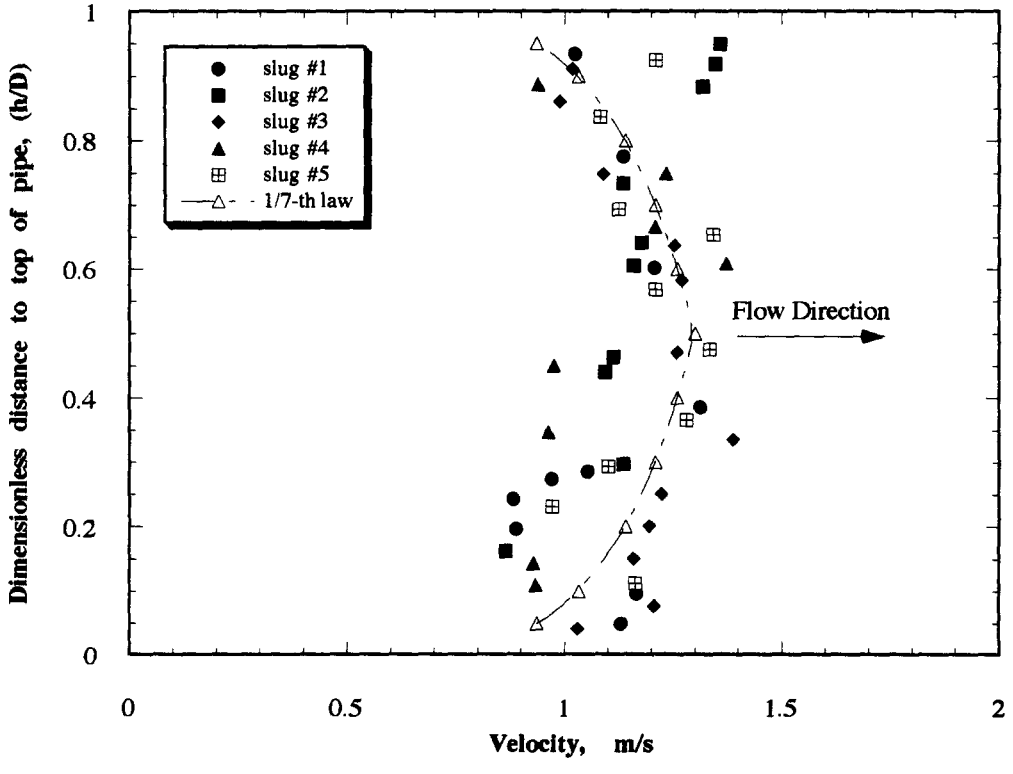

(b)

Figure 7. (a) and (b). *Continued overleaf.*

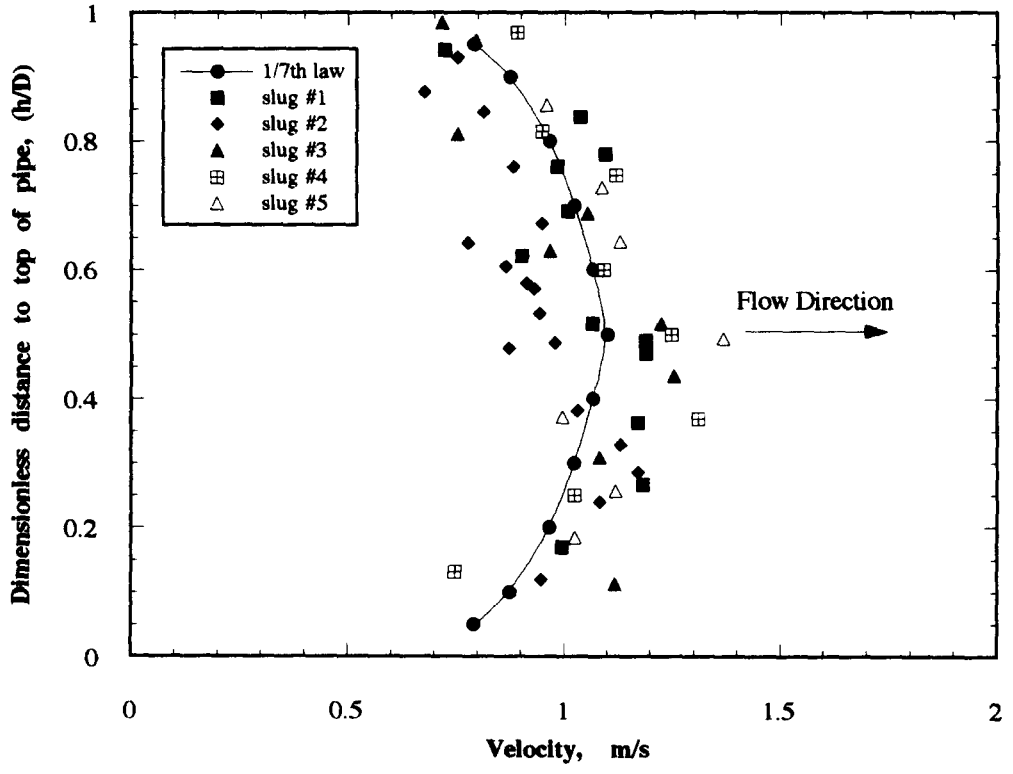

(c)

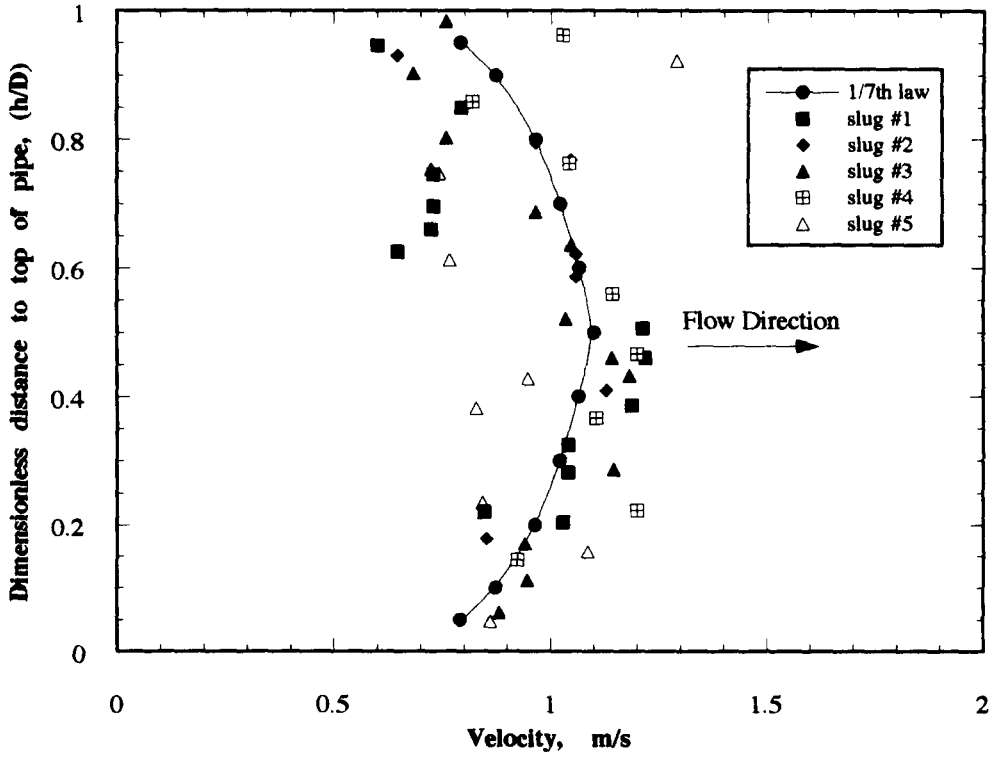

(d)

Figure 7. Velocity Profile (a) at the slug front, (b) 20 cm into slug, (c) 45 cm into slug, and (d) at the slug tail. $V_{SL} = 0.2$ m/s, $V_{SG} = 1.07$ m/s.

superficial gas and liquid velocities in each case (Jepson 1989). This result supports the assumptions made by Dukler *et al.* (1985).

3.2. *Transverse velocity in slug body*

Figure 8 shows the transverse velocity profiles at different distances in the slug body for a superficial liquid velocity of 0.2 m/s, and superficial gas velocity of 1.07 m/s. Due to buoyancy forces, the gas bubbles are pushed towards the top of the pipe and gives rise to a transverse velocity profile across the section of the pipe.

The transverse velocities are mostly in the range of 0–0.2 m/s. There are some transverse velocities that are negative, indicating that the bubbles have moved in a slightly downward direction. This is specially true near the slug tail due to the presence of the gas pocket which follows the slug tail. The gas tends to accelerate the liquid near the top of the pipe, causing a small downward motion towards the bottom of the pipe.

Figure 9 shows the variation of the average transverse or rise velocity as a function of distance into the slug for the same velocity. It is seen that there is very little variation in the average rise velocity with distance into the slug and this average lies around 0.07 m/s. The results are similar at other velocities.

3.3. *Void fraction distribution*

Figure 10 shows the void fraction distribution across sections of the pipe in the slug body for superficial liquid velocities of 0.2 and 0.4 m/s, and superficial gas velocities of 1.07 and 1.43 m/s, respectively.

It is seen that the void fraction increases in a nonlinear manner from the bottom to the top of the pipe. There is little difference in void fraction in the lower half of the pipe. In the upper half of the pipe, however, there is a significant increase in void fraction. This is expected, since at the end of the mixing zone, the gas moves towards to the top of the pipe due to buoyancy forces.

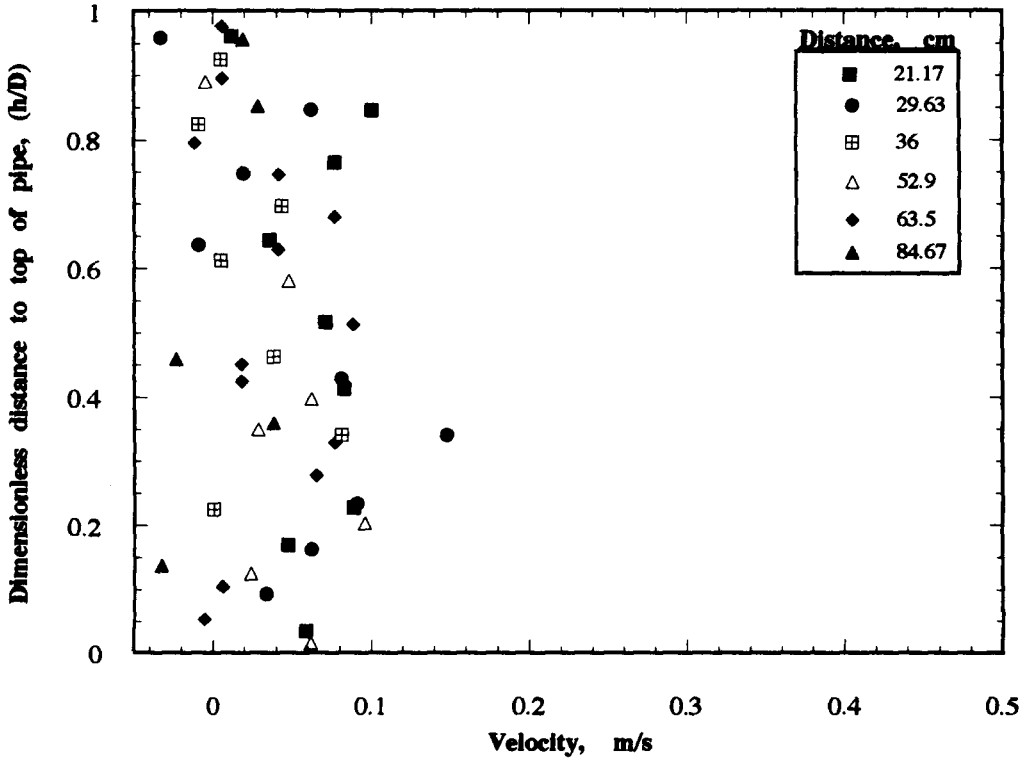

Figure 8. Transverse velocity profile at different distances into slug. $V_{SL} = 0.2$ m/s, $V_{SG} = 1.07$ m/s.

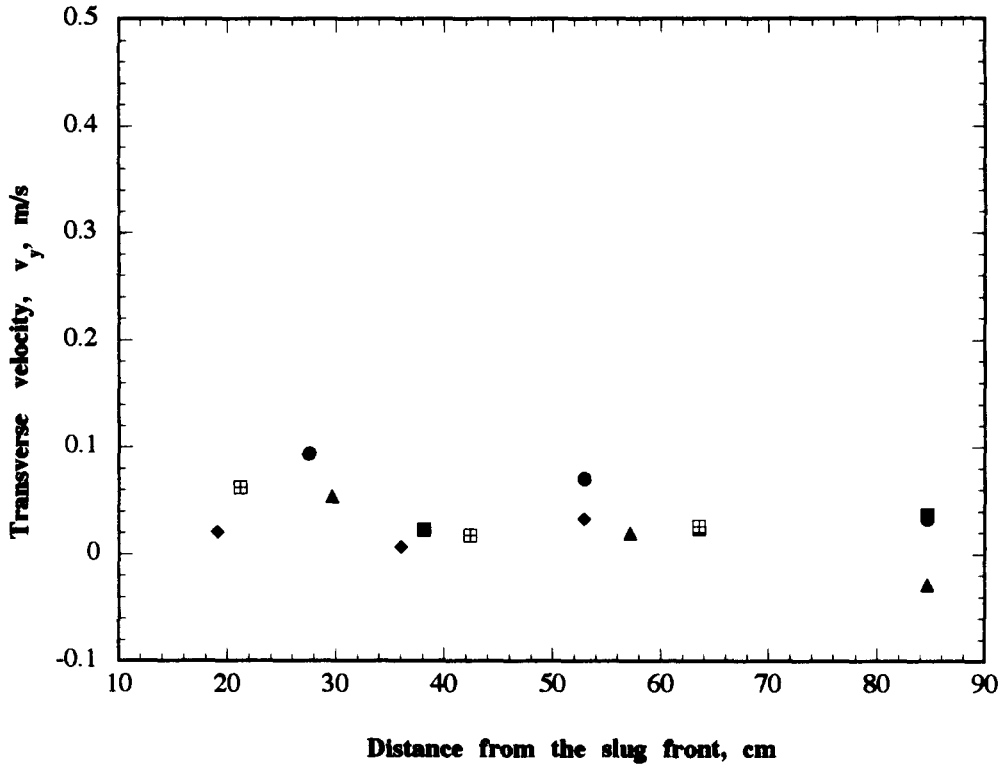

Figure 9. Average transverse velocity at different distances into slug. $V_{SL} = 0.2$ m/s, $V_{SG} = 1.07$ m/s.

However, the turbulence in the slug holds some gas bubbles in the mainstream of the flow. As noted before, most of the gas in this region of the slug is now distributed in the form of discrete bubbles.

It is seen from figure 10(a), that for a superficial liquid velocity of 0.2 m/s, and a superficial gas velocity of 1.07 m/s, the void fraction in the lower half of the pipe is less than 10%. It increases to about 20% at a h/D of 0.9, and then increases rapidly to values of 60–90% in the top tenth of the pipe.

Figure 10(a) also shows that the void fraction at the top of the pipe increases with distance into the slug. At a distance of 10 cm into the slug the void fraction at the top of the pipe is about 30%. This increases to about 50% at a distance of about 40 cm into the slug. Near the tail of the slug, at a distance of 75 cm, the void fraction increases to more than 80% at the top indicating that a thin gas film is formed, one of the characteristics of slug flow.

Figure 10(b) shows the void fraction variation for a superficial liquid velocity of 0.3 m/s, and a superficial gas velocity of 1.07 m/s. In this case the void fraction is less than 20% in the lower half of the pipe. It increases to about forty percent at a h/D of 0.8, and then increases to about 50–80% near the top of the pipe. This again shows the formation of a thin film of gas at the top of the pipe.

Figure 10(b) shows the void fraction variation for a superficial liquid velocity of 0.4 m/s, and a superficial gas velocity of 1.43 m/s. The trend is similar in this case but a higher void fraction is present in the lower sections of the pipe.

It is noted that all of the void profiles (over 150) at various distances in the slug body that were generated had the same shape as shown in figure 10(a) and (d). It is, therefore, reasonable to assume that they may be described by a single equation as follows

$$\epsilon(\bar{h}) = \frac{a\bar{h}}{(1 - b\bar{h})}, \qquad [8]$$

where $\bar{h}$ is the dimensionless distance, h/D from the bottom of the pipe.

A mean value of 0.1 for coefficient a and a value of 0.8–0.85 for the ratio of b/a are assumed

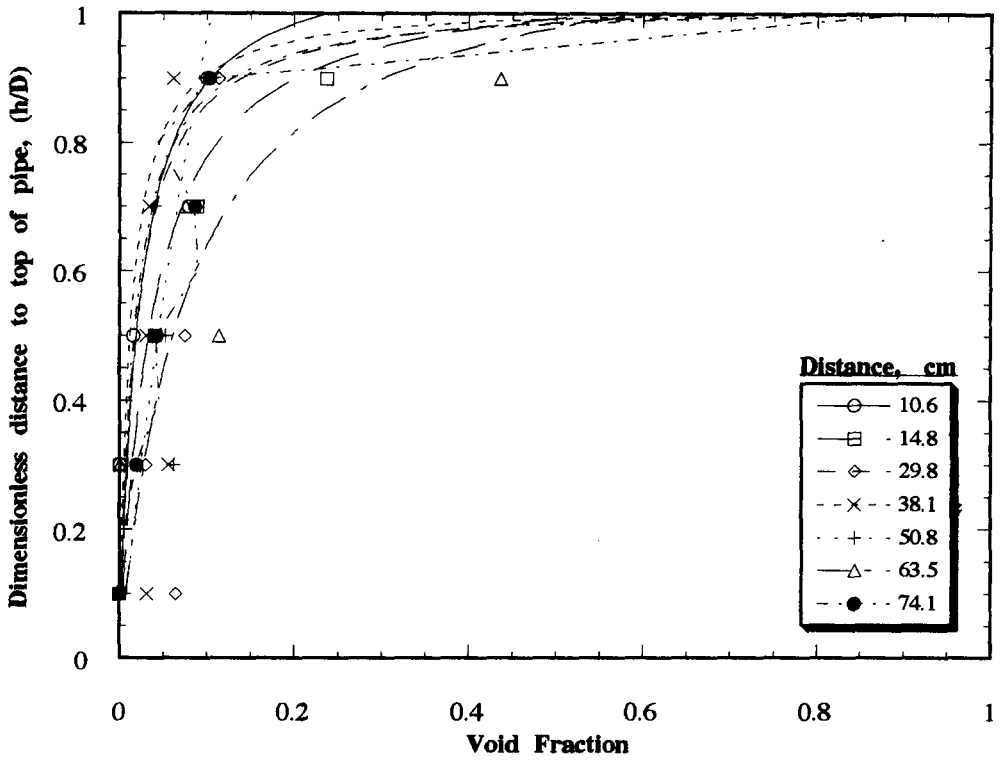

(a)

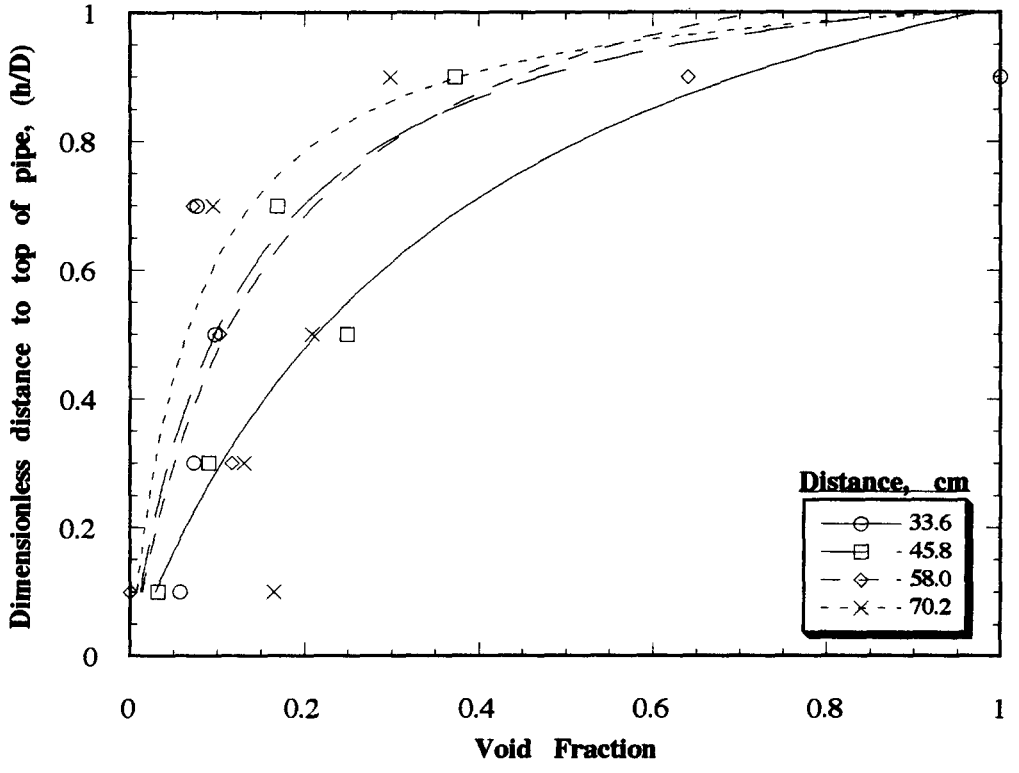

(b)

Figure 10. Void fraction profile across cross section of pipe in slug body water–CO_2 slug systems. (a) V_{SL} = 0.2 m/s, V_{SG} = 1.07 m/s, (b) V_{SL} = 0.4 m/s, V_{SG} = 1.43 m/s.

to be reasonable values to use to approximate the void fraction profile in the slug body for all cases. These are the recommended values to use with [8] for void fraction calculations in the slug body.

Jepson (1986) and Zhou *et al.* (1992) generated void fraction data for stationary slugs. The void fraction profiles given in figures 10(a) and (b), and [8] agree with the void profile given by these authors.

3.4. *Liquid holdup in slugs*

Liquid holdup in the slug is determined by subtracting the void fraction in the slug from unity. Figure 11 shows the variations of liquid holdup along the length of the slug. As is expected, the liquid holdup also increases in a nonlinear manner, from the front of the slug to the tail. The liquid holdup in the body of the slug tends towards a constant value.

Figure 11(a) shows the variation of the average liquid holdup across a cross section of pipe as a function of distance into the slug, for a superficial liquid velocity of 0.2 m/s, and a superficial gas velocity of 1.07 m/s. It is seen that the average liquid holdup varies substantially near the slug front. Values from 90% to as low as 30% are noted within the first 15 cm of the slug and corresponds to the flow in the mixing zone. Jepson (1987) showed that gas was entrained and released into the slug in form of pulses of bubbles at a definite frequency. This explains the variation in the liquid holdup in this region of the slug.

Kouba (1986) proposed that there is a maximum void fraction (or minimum liquid holdup) in the mixing zone. If it is assumed that bubbles assemble themselves in a manner similar to crystallization phenomena in metallic structures, then the concept of 'packing efficiency' in metals may be applied to the gas bubble arrangement. The maximum packing efficiency of a body centered cubic structure is 0.68, while that of a face centered cubic structure and a hexagonal close packed structure is 0.74. Therefore, he postulated that a maximum void fraction exists in the mixing zone somewhere around seventy percent. This is borne out for slug #3 in figure 11(a) and the video image in figure 6(a). Slug #3 provides void fraction data at the slug front within a pulse of bubbles. The liquid holdup increases to about 90% at 35 cm into the body of the slug. This also provides an insight into the reason for the change in velocity profile with distance into the slug body. When the void profile reaches a quasi-steady state, the liquid boundary layer is able to fully develop.

Figure 11(b) shows the variation of the average liquid holdup across a cross section of pipe as a function of distance, for a superficial liquid velocity of 0.3 m/s, and a superficial gas velocity of 1.43 m/s. In this case the oscillation of the liquid holdup near the slug front is much more pronounced. The liquid holdup oscillates between 45 and 75% before rising asymptotically to a value of 80%. It is seen from figure 11(d) that near the slug front, sinusoidal wave pattern exists for the liquid holdup. The remnants of this wave can be seen in the other cases as well, and the initial data point is not predicted by the fitted curve.

An inspection of the holdup variation within the slug for the various sets of velocities show that in all cases, these variations resemble the response of a second order system to a step input (Coughanour and Koppel 1982).

A second order process system is one that may be mathematically described by the following differential equation

$$\tau^2 \frac{d^2Y}{dt^2} + 2\zeta\tau \frac{dY}{dt} + Y = X(t). \qquad [9]$$

A second order process is usually characterized by a viscous damping force and an elastic spring constant. A classical example is the rheology of a viscoelastic fluid, and τ and ζ are usually some ratio of these forces.

The response of the second order system is dependent on the value of ζ. Three cases arise. For $\zeta < 1$, the response is given by

$$Y(t) = A\left[1 - \frac{1}{\sqrt{1-\zeta^2}} e^{-\zeta t/\tau} \sin\left(\sqrt{1-\zeta^2}\frac{t}{\tau} + \tan^{-1}\frac{\sqrt{1-\zeta^2}}{\zeta}\right)\right. \qquad [10]$$

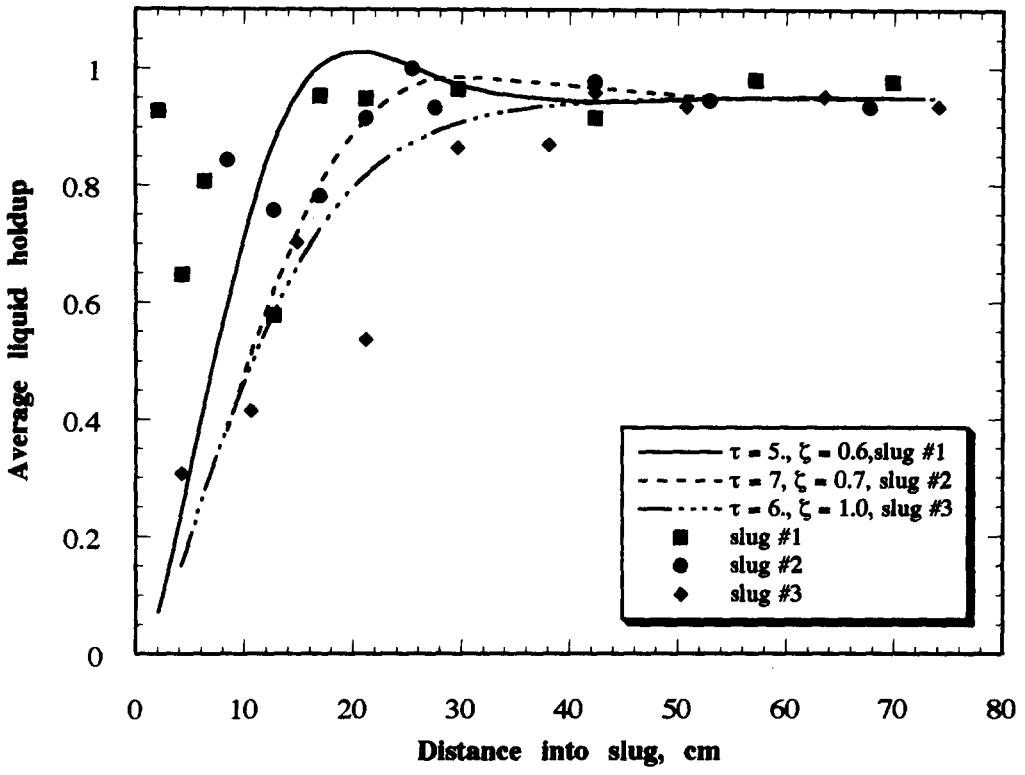

(a)

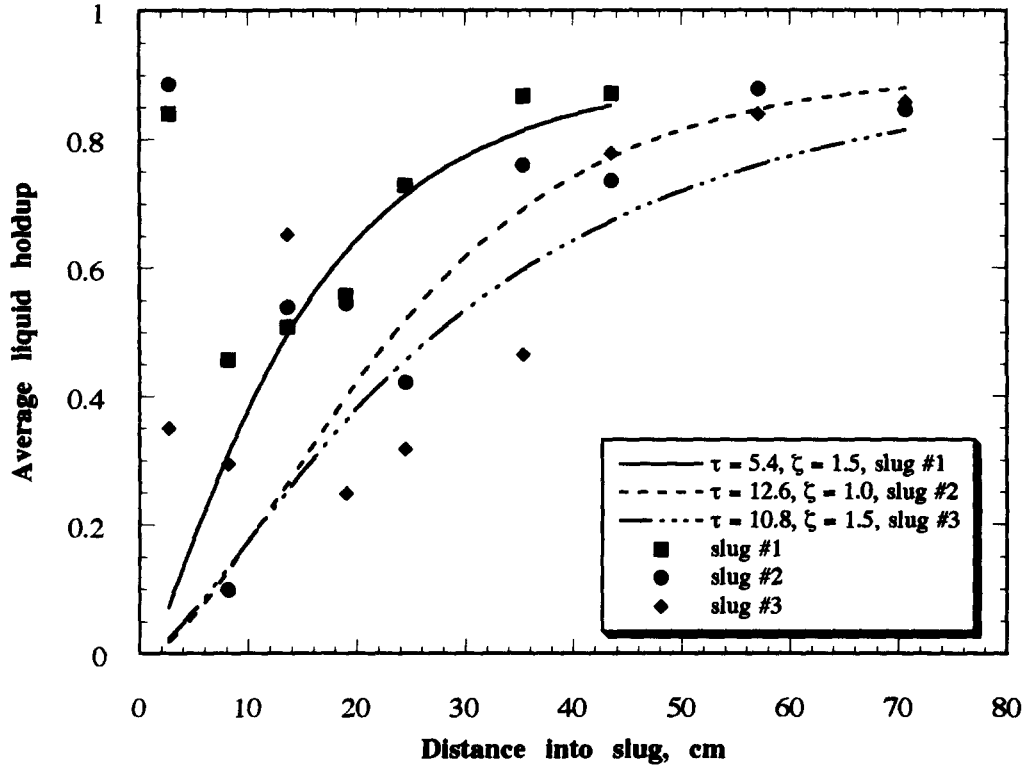

(b)

Figure 11. Model for liquid holdup variation in slug water–CO_2 slug system. (a) $V_{SL} = 0.2$ m/s, $V_{SG} = 1.07$ m/s, (b) $V_{SL} = 0.2$ m/s, $V_{SG} = 1.43$ m/s.

Table 2. Comparison between holdup model parameters and experimental values

Slug velocity(m/s)	Mean ζ	Model ζ	Mean τ	Model τ
1.27	1.16	0.75	6	7.1
1.37	0.8	0.93	6	5.7
1.63	0.74	0.71	5	4.34
1.73	1.3	1.1	9.6	5.4
1.83	0.76	0.87	6	6.5

$$Y(t) = A\left[1 - \frac{1}{\sqrt{1-\zeta^2}} e^{-\zeta t/\tau} \sin\left(\sqrt{1-\zeta^2}\frac{t}{\tau} + \tan^{-1}\frac{\sqrt{1-\zeta^2}}{\zeta}\right)\right]. \quad [10]$$

For the case when $\zeta = 1$, the response is

$$Y(t) = A\left[1 - \left(1 + \frac{t}{\tau}\right)e^{-t/\tau}\right], \quad [11]$$

and, for $\zeta > 1$, the response becomes

$$Y(t) = A\left[1 - e^{-\zeta t/\tau}\left(\cosh\sqrt{\zeta^2-1}\frac{t}{\tau} + \frac{\zeta}{\sqrt{\zeta^2-1}}\sinh\sqrt{\zeta^2-1}\frac{t}{\tau}\right)\right]. \quad [12]$$

If figure 11(a) and (b) are examined closely, it is found that the response curves defined by [10]–[12] fit the data for the liquid holdup in the slug very well. Jepson (1987) showed that the slug front is a hydraulic jump. It appears that the hydraulic jump at the slug front acts as a step input to the liquid film. The resultant variation of liquid film holdup in the slug then behaves as a second order system.

The values of ζ and τ were estimated by a best fit regression curve. In each case, an appropriate ζ value was used as an initial guess with the value of τ fixed. The value of ζ was then equated to

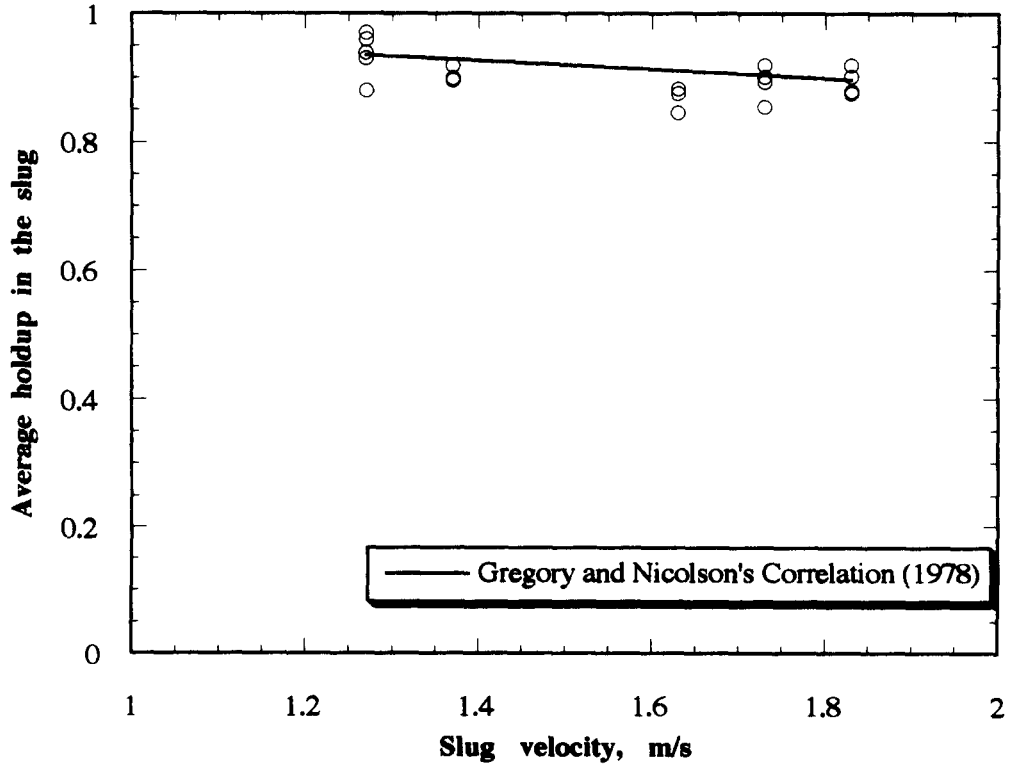

Figure 12. Variation of average liquid holdup in the slug with slug velocity.

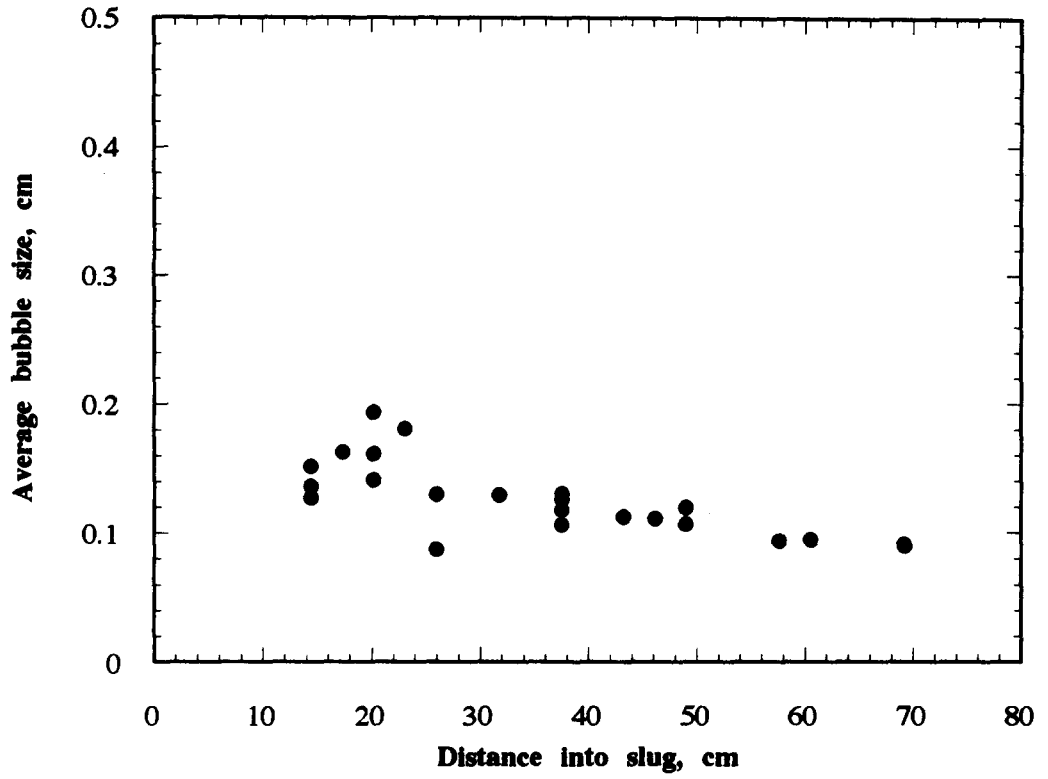

Figure 13. Variation of average bubble size with distance into slug water–CO_2 slug system. V_{SL} = 0.3 m/s, V_{SG} = 1.43 m/s.

ratios of dimensionless numbers characterizing the slug flow and τ was estimated as a fraction of the mixing length. The dimensionless numbers are the Reynolds, Eotvos and Froude numbers.

3.5. Definition of dimensionless numbers

Jepson (1987) defined the film Froude number and showed that this was the controlling parameter for slug flow. The film Froude number is given by:

$$\mathrm{Fr}_f = \frac{v_t - v_{LF}}{\sqrt{gh_{EF}}}. \qquad [13]$$

The effective height of the liquid film, h_{EF}, is given by the ratio of the area occupied by the liquid film divided by the width of the gas–liquid interface.

The Reynolds number and Eotvos number required for characterizing the liquid holdup variation are given by

$$\mathrm{Re}_{SL} = \frac{D v_{SL} \rho_L}{\mu_L} \qquad [14]$$

and

$$\mathrm{Eo} = \frac{g\rho_L D^2}{\sigma}, \qquad [15]$$

where D is the pipe diameter, v_{SL} is the superficial liquid velocity, and, ρ_L and μ_L are the density and viscosity of the liquid.

3.6. Estimation of ξ and τ

From the knowledge of the mixing length (Gopal *et al.* 1995) and the dimensionless numbers,

at any given slug velocity, the values of ζ and τ in [10]–[12] may be estimated as

$$\tau = \frac{L_m}{4}, \qquad [16]$$

$$\zeta = \frac{\mathrm{Fr_f}}{\sqrt{\mathrm{Re/Eo}}},$$

where L_m is the length of the mixing zone of the slug (Gopal *et al.* 1995).

Table 2 lists the comparison between the model estimations of ζ and τ with the mean values obtained by the nonlinear regression of the experimental data.

It is seen that there is good agreement between the experimental values and the theoretical model estimations. Further experiments are needed with other fluids before definite conclusions can be drawn. However, it is felt that there is a reasonable trend here, and that the liquid holdup variations in slug flow can be described using this concept.

Figure 12 shows a comparison of the liquid holdup calculated from this model and that predicted by the correlation of Nicholson *et al.* (1978) given by [1]. It is seen that there is very good agreement between the two cases.

3.7. Bubble diameters

An analysis of the bubble diameters within the slug body, for all the cases described above as a function of distance into the slug indicated that the bubble diameters in all the cases lay between 1 and 2 mm. Figure shows the variation of bubble diameters across the pipe section in the slug body for a superficial liquid velocity of 0.2 m/s and a superficial gas velocity of 1.07 m/s. The bubble diameters range from 1 to 2 mm.

4. CONCLUSIONS

Slug flow characteristics have been studied and modeled for two-phase gas–liquid systems in a 7.6 cm diameter pipe. The liquid superficial velocity ranged from 0.2 to 0.7 m/s and the superficial gas velocity ranged from 1 to 5 m/s.

A novel flow visualization system has been developed to study the detailed characteristics of slug flow. Digital image processing algorithms have been developed involving edge-tracking routines. The coordinates of bubbles and voids within the slug were obtained using these routines. These were then used to determine a velocity and void fraction profile across the entire cross section of the pipe at different distances into the slug.

Velocity profiles in slugs at velocities ranging from 1.27 to 1.83 m/s indicate that near the front of the mixing zone, there is a high degree of turbulence, resulting in the destruction of the hydrodynamic boundary layer and the development of a flat velocity profile. At the end of the mixing zone, the boundary layer has fully redeveloped and a one-seventh power law model provides a good estimate of the shape of the velocity profile in the slug. At the tail of the slug the effect of the gas pocket behind the slug begins to distort the boundary layer once more.

Different void structures in slugs were noted and these were divided into two types. In the mixing zone and near the top of the pipe were large voids that were distributed throughout the depth of the pipe. Beyond the mixing zone, discrete gas bubbles are formed and move towards the top of the pipe. The predominant form of voids in this region of the slug is spherical bubbles. Based on this classification, the void profile across the slug was computed. The data obtained using this technique were used to compute the overall void fraction and these agree well with the empirical model proposed by Gregory *et al.* (1978).

The void fraction distribution across a section of the pipe in the slug body was seen to have a steady profile, for all cases. The void fraction up to the center of the pipe was less than 10–15%. It then increased rapidly to values between 50 and 90% near the top of the pipe. A regression analysis was performed with over 200 images, and a single equation was proposed to describe the void fraction variation in the slug body.

The average liquid holdup in the slug was seen to vary substantially near the slug front from

about 70 to 30%. This was due to the release of pulses of bubbles in the mixing zone. At the end of the mixing zone, the holdup increased to a steady value of about 80–90%.

The holdup variation in slugs was modeled as the response of a second order viscoelastic system to a step input. A nonlinear regression fit was performed to obtain values of the process parameters, τ and ζ that characterize the system. A model was developed to predict the value of ζ using ratios of the Froude, Reynolds and Eotvos numbers. τ was modeled as being one-fourth of the mixing length. The model incorporates the effects of liquid density, viscosity, and surface tension on the liquid holdup. Model results show good agreement with experimental data.

REFERENCES

Andreussi, P., Bendiksen, K. H. and Nydal, O. J. (1993) Void distribution in slug flow. *Int. J. Multiphase Flow* **19,** 817–828.

Andreussi, P. and Bendikson, K. (1989) An investigation of void fraction in liquid slugs for horizontal and inclined gas–liquid pipe flow. *Int. J. Multiphase Flow* **6,** 937–952.

Barnea, D. and Brauner, N. (1985) Holdup of the liquid slug in two phase intermittent flow. *Int. J. Multiphase Flow* **11,** 43–49.

Barnea, D., Shoham, O. and Taitel, Y. (1982) Flow pattern transition for downward inclined two-phase flow, horizontal to vertical. *Chem. Engng Sci.* **37,** 135–140.

Cowghanowr, D. R. and Koppel, L. B. (1986) *Process Systems Analysis and Control.* McGraw-Hill, New York.

Dukler, A. E. and Hubbard, M. G. (1975) A model for gas–liquid slug flow in horizontal and near horizontal tubes. *Ind. Eng. Chem. Fundam.* **14,** 337–347.

Dukler, A. E., Maron, D. M. and Brauner, N. (1985) A physical model for predicting the minimum stable slug length. *Chem. Engng Sci.* **40,** 1379.

Fairhurst, C. P. (1988) Slug-flow behavior clarified in large diameter pipeline study. *O. G. J.*, 49–61.

Ferschneider, G. (1983) Revue de L'Institut Francais du Petrole, Vol. 38, p. 153.

Gopal, M., Kaul, A. and Jepson, W. P. (1995) Mechanisms contributing to enhanced corrosion in horizontal three phase slug flow. NACE/95, paper no. 105, pp. 1–16, NACE, Houston, TX.

Gregory, G. A., Nicholson, M. K. and Aziz, K. (1978) Correlation of the liquid volume fraction in the slug for horizontal gas–liquid slug flow. *Int. J. Multiphase Flow* **4,** 33–39.

Jepson, W. P. and Taylor, R. E. (1993) Slug flow and its transitions in large-diameter horizontal pipes. *Int. J. Multiphase Flow* **119,** 411–420.

Jepson, W. P. (1989) Modelling the transition to slug flow in horizontal conduit. *Canada J. Chem. Engng* **67,** 731–740.

Jepson, W. P. (1987) The flow characteristics in horizontal slug flow. *3rd Int. Conf. Multiphase Flow* Paper F2, pp. 187–197.

Kouba, G. E. (1986) Horizontal slug flow modelling and metering. Ph.D. thesis, University of Tulsa.

Kouba, G. E. and Jepson, W. P. (1990) The flow of slugs in horizontal, two-phase pipelines. *Trans. ASME* **112,** 20–24.

Maron, D. M., Yacoub, N. and Brauner, N. (1982) New thoughts on the mechanisms of gas–liquid slug flow. *Lett. Heat Mass Transfer* **9,** 333–341.

Taitel, Y. and Dukler, A. E. (1976) A model for predicting flow regime transitions in horizontal and near horizontal gas–liquid flow. *AIChE J.* **22,** 47–55.